Pannexin-1 mediates large pore formation and interleukin-1ß release by the ATP-gated $P2X_7$ receptor

Pablo Pelegrin and Annmarie Surprenant*

Department of Biomedical Science, University of Sheffield, Sheffield, UK

*Corresponding author. Department of Biomedical Science, University of Sheffield, Western Bank, Sheffield, South Yorkshire S10 2TN, UK. Tel.: þ 44 114 222 2366; Fax: þ 44 114 222 2360;

E-mail: a.surprenant@shef.ac.uk

Abstract

P2X7 receptors are ATP-gated cation channels; their activation in macrophage also leads to rapid opening of a membrane pore permeable to dyes such as ethidium, and to release of the pro-inflammatory cytokine, interleukin-1β (IL-1β). It has not been known what this dye-uptake path is, or whether it is involved in downstream signalling to IL-1β release. Here, we identify pannexin-1, a recently described mammalian protein that functions as a hemichannel when ectopically expressed, as this dye-uptake pathway and show that signalling through pannexin-1 is required for processing of caspase-1 and release of mature IL-1β induced by P2X7 receptor activation.

Keywords: hemichannel; inflammasome; ion channel; pro-inflammatory cytokines; purine receptors

Introduction

Interleukin-1β (IL-1β) is considered the initiator of the acute inflammatory response (Dinarello, 2005). Bacterial endotoxins and other inflammatory stimuli initiate its synthesis as a 31 kDa, biologically inactive, precursor molecule (pro-IL-1β), which can then be cleaved to the bioactive 17kDa mature IL-1β by proteolytically active caspase-1 (Martinon and Tschopp, 2004; Dinarello, 2005; Ferrari et al, 2006). However, in the absence of a secondary stimulus, the processing and release of bioactive IL-1β is extremely inefficient. For example, more than 95% of the pro-IL-1β induced by the endotoxin lipopolysaccharide (LPS) remains unprocessed and dispersed throughout the cytoplasm until a secondary stimulus rapidly (within 2–5 min) induces the processing and release of bioactive IL-1β (Perregaux and Gabel, 1994; Mackenzie et al, 2001; Kahlenberg and Dubyak 2004; Ferrari et al, 2006). While viral and bacterial elements can subserve this role (Martinon and Tschopp, 2004; Dinarello, 2005), the only known physiological stimuli for this rapid processing and release of bioactive IL-1β are allogenic cytotoxic T cells and activation of the ATP-gated P2X7 receptor (P2X7R) (Perregaux and Gabel, 1994; Perregaux et al, 1996; Mackenzie et al, 2001; Kahlenberg and Dubyak 2004; Ferrari et al, 2006).

The P2X7R, expressed on macrophage and other immune cells, is an ion channel gated by high concentrations of extracellular ATP, concentrations that are known to be present at sites of injury and inflammation (North, 2002; Ferrari et al, 2006). Recent studies using transgenic mice lacking the P2X7R have most clearly demonstrated that this plasma membrane protein is directly responsible for ATP-mediated processing and release of IL-1β from LPS-primed cells (Solle et al, 2001). These mice also exhibit altered bone formation and decreased inflammatory responses (Solle et al, 2001; Ke et al, 2003), making the P2X7R an attractive new target for anti-inflammatory drug

discovery. Molecular mechanisms by which P2X7R activation couples to IL-1β processing and release remain unclear.

The P2X7R is unique among ion channels in that its activation not only opens a 'typical' ion channel selective for small cations including calcium but also leads to the gradual opening over seconds to minutes of a larger pore that allows passage of molecules up to 900 Da (North, 2002; Ferrari et al, 2006). The 'large pore' properties of this receptor are usually assayed by uptake of fluorescent dyes such as ethidium and YoPro1 (North, 2002). Conventionally, it had been thought that the ion channel itself dilated to allow dye uptake; however, several recent studies have concluded that a distinct protein, or proteins, activated by P2X7Rs, more likely form this dye-uptake path (Schilling et al, 1999; North, 2002; Faria et al, 2005; Jiang et al, 2005). It is not known whether this dye-uptake path plays a role in immune cell function but identification of a distinct P2X7-activated large pore, if present, should lead to significant new insight into the mechanisms underlying ATP-gated IL-1β release.

We initially sought this putative P2X7R-activated pore by asking whether we could find a common membrane protein present in macrophage and macrophage-like cell lines that also could form a protein–protein interaction with the P2X7R and show functional properties of a dye-uptake pore. We hypothesized that a possible candidate may be a non-selective hemichannel pore. Two unrelated protein families could fulfil such a role: connexins or pannexins. Connexins are a multigene superfamily of proteins well known to form gap junctions; gap junctions are formed between cells by docking of connexin hemichannels, which are thought to exist as undocked oligomers prior to junctional formation (Spray et al, 2002; Dhein, 2004; Griffith et al, 2004). However, several previous studies have ruled out involvement of connexins in P2X7R activation and dye uptake (Steinberg and Di Virgilio, 1991; Hickman et al, 1996). Pannexins are

a recently identified three-membered family (Panx1, Panx2, Panx3) of mammalian proteins that have low sequence homology, but general structural similarity, to a family of non-mammalian proteins (innexins) that form gap junctions in invertebrate tissue (Panchin, 2005; Barbe et al, 2006). Although no functional role for these proteins has been demonstrated in situ, ectopic expression of Panx1 cDNA in oocytes results in hemichannel-like membrane currents that can act as a conduit for release of intracellular ATP in single oocytes and the formation of junctional coupling between panx1 overexpressing oocytes (Barbe et al, 2006). Moreover, very recent data have provided indirect evidence that panx1 may be responsible for ATP release from erythrocytes in response to mechanical or osmotic stimulation (Locovei et al, 2006a). Here, we find that panx1 is highly expressed in human and mouse macrophage, is upregulated by LPS stimulation, and co-immunoprecipitates with the P2X7R protein. Selective inhibition of panx1 by small interference RNA (siRNA) targetting panx1 and by a panx1-mimetic inhibitory peptide inhibited P2X7R-mediated dye uptake without altering the associated membrane current or calcium influx, and without altering P2X7R protein expression. Overexpression of panx1 increased the rate of P2X7R-mediated dye uptake and induced constitutive dye-uptake in the absence of P2X7Rs. Inhibition of panx1 with siRNA or the panx1-mimetic inhibitory peptide blocked caspase-1 cleavage as well as IL-1β processing and release from a repertoire of LPS-primed mouse and human macrophage in response to P2X7R activation. Thus, we have identified panx1 as the large pore pathway activated by P2X7Rs and as an upstream molecule essential for activation of the caspase-1/IL-1β inflammasome from activated macrophage by this receptor.

Results

Panx1 tissue expression and association with P2X7R

We used RT–PCR and quantitative RT–PCR (qPCR) to examine panx1 expression in a variety of immune cells and cell lines; we found high levels of mRNA for panx1 in human and mouse monocyte, macrophage and astrocyte cells and cell lines (Figure 1A). It was also present in non-immune cell lines (HEK, HeLa), which are extensively used to study heterologously expressed P2X7Rs. Phorbol esters, which up-regulate expression of P2X7Rs in macrophage (Humphreys and Dubyak, 1998), increased panx1 mRNA by four- to six- fold with further significant increased expression after LPS stimulation (Figure 1β). Because of these findings, and because a non-junctionally coupled hemichannel might be able to function as a dye-permeable pore (Barbe et al, 2006; Locovei et al, 2006a), we considered panx1 a potential candidate for a role in P2X7R-mediated dye uptake. We therefore cloned human panx1 from activated THP-1 macrophage (Supplementary Figure 1A), transiently overexpressed an epitope-tagged Panx1 protein in P2X7-expressing HEK cells and found that panx1 protein co-immunoprecipitated with P2X7Rs (Figure 1C). When transfected into HEK or HeLa cells, the panx1 protein was localized to the plasma membrane (Figure 1D, left-hand panel).

Activation of P2X7Rs induces rapid cytoskeletal re-arrangement of actin and other adhesion molecules, which leads to extensive membrane blebbing within 30–120 s (Mackenzie et al, 2001, 2005; Morelli et al, 2003). P2X7R-induced membrane blebbing is readily reversible when receptor activation is relatively brief (o10–15min) and the P2X7R protein can be seen to remain in the plasma membrane of the blebs as they swell and then retract (Mackenzie et al, 2001, 2005; Morelli et al, 2003). Overexpressing a GFP-fused Panx1 protein, we observed identical localization during

P2X7R mediated membrane blebbing; that is, panx1 tracked identically in time and space with P2X7 protein during the formation and retraction of membrane blebs (Figure 1D, right-hand panel).

Panx1 inhibition selectively blocks P2X7R induced dye-uptake

We generated a series of siRNAs targeting Panx1 and synthesized several peptides mimicking residues in the ectodomain of panx1 in an attempt to selectively inhibit the expression and/or function of this protein (Supplementary Figure 1A and B). One of the siRNA constructs (siRNA70) was highly effective in knocking down endogenous expression of panx1 mRNA in HEK cells and THP-1 macrophage (Figure 1E). It also completely blocked exogenous expression of panx1 protein without altering protein levels of P2X7R (Figure 1F).

Panx1 siRNA70, but not scrambled siRNA or other panx1 targeted siRNAs, markedly inhibited the rate and magnitude of ATP-induced YoPro1 or ethidium uptake without altering membrane currents (Figure 2A, C and D). The selective inhibition of dye-uptake was unequivocally evidenced by simultaneous recording of membrane currents and ethidium fluorescence from single cells during whole-cell patch-clamp experiments (Figure 2A). We also generated complete ATP concentration–response curves for membrane currents and measured maximum current density in cells treated with scrambled siRNA or siRNA70. In the same population of cells in which siRNA70 inhibited ATP-mediated dye-uptake by 60–100% (n = 6 experiments), no significant change in ATP EC50 at membrane currents (EC50 = 215 ± 22 μM scrambled siRNA versus 201 ± 35 μM siRNA 70, n = 4) or ATP-evoked maximum currents (145 ± 37 pA/pF, n = 14 scrambled siRNA versus 129 ± 42, n = 9 siRNA 70) were observed (Figure 2A and F).

We similarly examined the actions of several panx1- mimetic peptides and found one, 10panx1, (Supplementary Figure 1β and C) that potently inhibited P2X7-mediated dye uptake without altering other aspects of P2X7R activation (Figure 2B, E and F). The generation of this panx1-mimetic inhibitory peptide was of particular significance as it allowed us to readily and reliably examine inhibition of panx1 in cells in which efficient and consistent delivery of siRNA was extremely difficult (e.g. mouse J774 macrophage and alveolar macrophage obtained from human lung resections; Figure 2E and F). ATP-evoked dye-uptake was inhibited within 5–10min exposure to 10panx1 in HEK cells transfected with rat or human P2X7Rs (Figure 2B and F), in mouse J774 macrophage and human lung alveolar macrophage (Figure 2E and F), as well as in human THP-1 macrophage and HeLa or 1321-N1 astrocytes transfected with a rat P2X7 expression vector (data not shown). In none of these cells did 10panx1 alter ATP-evoked membrane currents, ATP concentration–response curves (Figure 2B and F), or cytosolic calcium transients (data not shown). These results rule out the possibility that panx1 siRNA or 10panx1 peptide inhibit ATP-evoked dye-uptake by inhibition of the P2X7R or ion channel per se. Moreover, inhibition of panx1 did not significantly alter the kinetics or magnitude of ATP-evoked membrane blebbing (n = 8), or phosphatidylserine exposure as assayed by annexin-V-FITC binding (n = 3) (Mackenzie et al, 2001; Suadicani et al, 2006). Neither panx1 siRNA nor the panx1 inhibitory peptide altered membrane properties of HEK, HeLa or J774 cells (resting conductance, membrane capacitance and current–voltage relations). All experiments described above were carried out on physically isolated, uncoupled cells, but we also examined the effects of panx1 siRNA and 10panx1 peptide on electrical coupling in clusters of HEK293 cells. No change in membrane capacitance occurred in the presence of panx1 inhibition by either siRNA (n = 12) or 10panx1 peptide (200 mM, n

= 4), whereas the nonspecific gap junction blocker heptanol (200mM) reversibly abolished junctional coupling within 5 min (membrane capacitance before/after hepatanol 68 ± 3 pF/ 11 ± 0.7 pF, n = 5). The specific connexin 32-mimetic inhibitory peptide, gp27 (300mM) (Gudipaty et al, 2003), partially reduced electrical coupling (capacitance before/after 59 ± 4 pF/26 ± 3 pF, n = 4) in similar clusters of HEK cells. These control experiments confirm the specificity of the panx1 siRNA and peptide mimetic, and also rule out involvement of panx1 in formation of gap junctions in these cells.

Panx1 is a non-selective hemichannel when overexpressed in mammalian cells

Ectopic expression of panx1 in oocytes results in the appearance of hemichannel-like currents (Bao et al, 2004; Bruzzone et al, 2005; Panchin, 2005; Barbe et al, 2006). The existence of similar endogenous hemichannel currents in nonjunctional cells has not been reported, and nor have we observed similar currents, or constitutive dye uptake, in human or mouse macrophage, or any cell line we have used for transfection of P2X7Rs (Figure 3A and C). Thus, if indeed, such a non-selective hemichannel is involved in P2X7R dye-uptake, it must be nonfunctional in the absence of receptor activation. Therefore, we asked whether overexpression of panx1 protein resulted in hemichannel-like function in mammalian cells. Overexpression of panx1 protein in P2X7R-negative HEK or Hela cells resulted in a constitutive uptake of ethidium that was approximately 5–20% of the ATP-evoked ethidium up-take observed in P2X7-expressing cells (Figure 3A). In contrast, when panx1 was overexpressed in P2X7-positive cells, there was no constitutive ethidium uptake but the rate of dye uptake in response to ATP was significantly increased (slope of fluorescence increase = 40 ± 1 for panx1 overexpression versus 29 ± 2.5 for vector transfected, n = 4; Figure 3B).

Panx1 overexpression in P2X7 expressing cells did not alter ATP-induced membrane currents recorded at -60mV (no significant difference in ATP concentration–response or maximum current density; n = 12). These results suggest that unstimulated P2X7R may negatively regulate panx1 function.

Overexpression of panx1 in non-P2X7 expressing cells resulted in the appearance of membrane currents similar in most respects to those observed in previous studies using the oocyte expression system (Bao et al, 2004; Bruzzone et al, 2005; Barbe et al, 2006). These currents were activated by depolarization, and showed a nonselective ionic permeability profile (currents were unaltered by replacing sodium with the larger cation, NMDG, or with K^+ , Ca^{2+} or choline and they were also unaltered by changes in intracellular or extracellular Cl^-, n = 6 for each condition; Figure 3C and E). In agreement with results from oocyte studies (Bruzzone et al, 2005), panx1-mediated currents were effectively blocked by relatively low concentrations of the nonspecific gap-junction blocker, carbenoxolone (CBX; Figure 3C and E), but not by other generally used connexin channel/gap junction blockers (heptanol, mefloquine and connexin-mimetic inhibitory peptide gp27; Figure 3E). They were also unaffected by high concentrations of lanthanum or gadolinium (0.1–1 mM; Figure 3C and E). The panx1-currents were readily and reversibly blocked by the selective panx1-mimetic inhibitory peptide 10panx1 (Figure 3D and E). Steady-state inhibition by 10panx1 required 4–15 min. Concentration–inhibition curves were obtained for the actions of 10panx1 in inhibiting P2X7-mediated dye uptake and in inhibiting panx-1 mediated currents in panx-1 overexpressing cells; in both assays a similar half-maximal inhibitory concentration was obtained (30–50 mM; Supplementary Figure 2A). These concentrations are within the range (50–1000mM) typically seen to be effective in other systems where peptide-mimetic inhibitors are commonly used (Hickman et al,

1996; Gudipaty et al, 2003; Mariathasan et al, 2004; Elliott et al, 2005). Steady-state inhibition by an IC50 concentration of 10panx1 required 10–20 min with washout being accomplished within 15–25 min (n = 4).

We also examined the actions of the nonspecific gap junction/hemichannel blockers on P2X7R mediated responses in our repertoire of immune and nonimmune cells in the absence of panx1 overexpression. CBX, but not heptanol, mefloquine or gp27, selectively inhibited the ATP-evoked dye uptake in all these cells (Figure 4A, D and E). In contrast, CBX produced a small, but significant increase in the associated ATP-evoked membrane currents and cystosolic calcium transients (Figure 4A and B). The selective inhibition of P2X7-mediated dye-uptake by CBX occurred over the same concentration range as did the CBX inhibition of the panx1-mediated currents in panx1-overexpressing cells with half-maximal inhibition occurring at 2–4mM CBX (Figure 4D). These results not only conclusively rule out involvement of connexins in P2X7R-induced dye-uptake but also suggest the inhibition of ATP-evoked dye-uptake by CBX may be due to inhibition of panx1. It is important to emphasize that all our experiments were carried out only on physically isolated, electrically uncoupled cells, thus obviating any complications due to junctional coupling between cells. In this regard, a recent study using confluent, electrically coupled, 1321-N1 astrocytes expressing P2X7Rs found that CBX, heptanol and mefloquine all equally inhibited ATP-evoked dye-uptake and cytosolic calcium transients, and concluded that these nonselective connexin channel blockers acted as P2X7R antagonists (Suadicani et al, 2006). However, recordings of membrane currents, calcium transients and dye-uptake in physically isolated, single, 1321-N1 astrocytes transfected with P2X7R clearly show that none of these nonselective connexin channel blockers inhibit P2X7Rs (Figure 4B, C and E).

Panx1 is required for release of mature IL-1β in response to P2X7R activation

We next asked whether panx1 contributes to the physiological response in immune cells by measuring IL-1β release and processing from LPS-primed mouse J774 macrophage, human THP-1 cells and acutely isolated alveolar macrophage from human lung in response to P2X7R stimulation. Panx1 protein knockdown using siRNA70 transfection in human THP-1 cells significantly inhibited ATP-mediated IL-1β release while similar treatment with scrambled siRNA did not (Figure 5A). Neither of these siRNAs stimulated IL-1β release in the absence of P2X7R stimulation (Figure 5A).

The panx1-mimetic inhibitory peptide, 10panx1, blocked ATP-mediated IL-1β release in mouse and human macrophage (Figure 5B–D); we also confirmed that the actions of ATP to induce IL-1β release were due to P2X7R activation by the use of the anti-P2X7R monoclonal antibody (Figure 5B). CBX also significantly inhibited ATP-mediated release from these macrophages although maximal inhibition by CBX was not as effective as 10panx1 (Figure 5B). We used the connexin-mimetic inhibitor, gp27 (Spray et al, 2002; Dhein, 2004), to confirm the lack of involvement of connexins and also as a control peptide; this peptide resulted in a small, but significant, increase in amounts of IL-1β secreted into the medium (Figure 5B). As expected from much previous work (Perregaux and Gabel, 1994; Mackenzie et al, 2001; Gudipaty et al, 2003; Kahlenberg and Dubyak, 2004; Ferrari et al, 2006), the IL-1β released into the medium by activation of P2X7Rs was primarily the fully processed, 17kDa form, although the unprocessed 31 kDa form was also often present in the medium as well (Figure 6A–C); however, no 17kDa band was present in the medium after ATP

stimulation when cells were incubated with 10panx1 (Figure 6A–C) or with CBX (Figure 6B).

Because intracellular potassium depletion has been hypothesized as the underlying mechanism responsible for P2X7R-mediated release of bioactive IL-1β (Perregaux and Gabel, 1994; Martinon and Tschopp, 2004; Dinarello, 2005; Ferrari et al, 2006), we asked whether inhibition of pannexin altered K^+ levels by direct measurement of cellular and released potassium from J774 cells during our cytokine release protocols. In agreement with previous studies (Perregaux and Gabel, 1994; Perregaux et al, 1996; Kahlenberg and Dubyak, 2004), we found that ATP reduced intracellular K^+ by approximately 50% in LPS-primed cells with concomitant increased potassium in the medium, but the panx1-mimetic inhibitory peptide did not alter the P2X7R-mediated intracellular K^+ depletion (Figure 6D). Thus, intracellular K^+ depletion per se is not sufficient to induce P2X7R-evoked processing and release of IL-1β from LPS-primed macrophage.

Panx1 is required for caspase-1 cleavage in response to P2X7R activation

Finally, we asked whether panx1 may be involved further upstream in the caspase cascade using immunoblot assays of caspase-1. We compared actions of 10panx1 inhibitory peptide with actions of the selective caspase-1 inhibitor, Ac-YVAD-AOM, which blocks caspase-1 cleavage and subsequent caspase-1 dependent processing and release of IL-1β (Nemeth et al, 1997). Both 10panx1 peptide and Ac-YVAD-AOM abolished ATP-mediated intracellular cleavage of caspase-1 as evidenced by absence of the caspase-1 p10 fragment in cells incubated with either of these compounds (Figure 7A), as well as IL-1β release of mature IL-1β into the medium (Figure 7B). Lactate dehydrogenase (LDH) release was also measured in each caspase and

cytokine release experiment as an assay for cell death but under no condition did LDH levels change significantly (Supplementary Figure 2B).

Discussion

While dye-uptake has been a defining feature of, and useful assay for, the P2X7R for decades (precloning designated P2Z receptor), molecular mechanisms underlying this process and whether it relates to immune cell function have remained unknown (Perregaux and Gabel, 1994; Hickman et al, 1996; North, 2002; Ferrari et al, 2006). A functional link between P2X7R-activated large pore formation and cytokine release in macrophage has long been postulated (see Ferrari et al, 2006); here we show that pannexin-1 is this functional link. Selective blockade of panx1 protein with panx1 siRNA or the panx1-mimetic inhibitory peptide revealed the essential role of this membrane protein in P2X7R-activation of the caspase-1 cascade. Our results suggest that panx1 may act as a nonselective hemichannel activated by P2X7R stimulation and that it is this hemichannel activity, rather than ion flow through the P2X7R channel itself, that is responsible for activation of the caspase-1 cascade through the recently identified cryopyrin inflammasome (Mariathasan et al, 2006) in macrophage.

Early studies of ATP-activated dye uptake in macrophage had suggested that connexin hemichannels, which are permeable to molecules up to about 1000Da, were themselves the P2Z/P2X7R (Beyer and Steinberg, 1991). This idea was ruled out by the molecular identification of the P2X7R as a member of the P2X family of ion channels (North, 2002) and by results showing that ATP does not induce dye-uptake in P2X7-receptor negative cells where connexin proteins are endogenously expressed or heterologously overexpressed (Steinberg and Di Virgilio, 1991). Subsequently, two hypotheses have emerged to account for the dye-uptake: intrinsic P2X7R channel dilatation from cation-selective small channel to nonselective big pore or P2X7-receptor activated recruitment of an accessory pore-forming mechanism (Schilling et al, 1999; North, 2002; Faria et al, 2005; Jiang et al, 2005). The present results

decisively support the latter conclusion and identify panx1 as the critical accessory molecule. Selective inhibition of panx1 expression by siRNA knock-down blocked P2X7-mediated dye-uptake independently of P2X7R activation; similar results were obtained with the specific panx1-mimetic inhibitory peptide. Overexpression of panx1 in mammalian cells resulted in the appearance of depolarization-evoked membrane currents that exhibited biophysical properties previously associated with hemichannel function (non-selective anion/cation permeability to molecules <1 kDa) (Spray et al, 2002; Dhein, 2004; Griffith et al, 2004; Bruzzone et al, 2005) as well as constitutive ethidium uptake in P2X7-negative cells. The biophysical properties (large cation permeability) of the overexpressed pannexin-1 currents matched the properties of the ATP-evoked dye uptake pathway in P2X7R-expressing cells. However, these currents were observed only with overexpression of panx1 but not in cells in which only endogenous levels of panx1 were present. If panx1 does function directly as a hemichannel, these findings indicate that panx1 is nonfunctional in the absence of P2X7R stimulation. Our data are compatible with a negative regulation of panx1 activity by unstimulated P2X7Rs, in that constitutive dye uptake was observed when panx1 was overexpressed in P2X7R-negative cells but not in P2X7R-positive cells even though dye uptake was significantly increased by P2X7R activation in the same cells. Overall, our data suggest that the panx1 protein, acting as a plasma membrane hemichannel, is in fact the dye-uptake pore. However, we cannot rule out an alternative possibility that panx1 allows dye uptake by altering the function of plasma membrane lipids and membrane transporters in light of our recent study showing that P2X7R activation in T-lymphocytes leads to a reversal of activity of the multidrug efflux transporter, MDR/p-glycoprotein, via alterations in membrane lipids (Elliott et al, 2005).

While is it well known that gap junctions form by the docking of two connexin hemichannels from opposing faces of adjacent plasma membranes, it has been a matter of much debate as to whether open (unopposed) hemichannels have a functional role in non-junctional cells (Dhein, 2004; Locovei et al, 2006a). Most recently, hemichannel-like activity has been reported in hippocampal neurones in response to oxygen/glucose deprivation, and this activity was suggested to be consistent with activation of panx1 hemichannels, a conclusion based on inhibition by carbenxolone and lanthanum (Thompson et al, 2006). It is unlikely that panx1 hemichannels are responsible for the current observed in hippocampal neurones because we found that lanthanum had no effect on panx1-mediated currents or dye-uptake and panx1 current–voltage curves obtained in our study, and in previous studies on panx1 expression in oocytes, differ from the observed hemichannel activity in hippocampal neurones. However, panx2 is also found in hippocampal neurones and ectopically expressed panx1 and panx2 can form heteromic channels in oocytes with distinct biophysical properties (Barbe et al, 2006). Further studies, particularly making use of the selective panx1-mimetic inhibitory peptide we have identified, may reveal whether a heteromeric panx1/2 channel may underlie this neuronal hemichannel activity.

The mechanisms underlying the upregulation and synthesis of IL-1β in response to Toll like receptor (TLR) activation by LPS and the steps in its processing via the caspase cascade are fairly well understood (Martinon and Tschopp, 2004; Dinarello, 2005; Ferrari et al, 2006). LPS activation of TLR triggers synthesis of pro-IL-1β and its cytoplasmic accumulation. Further secondary stimuli, particularly P2X7R activation by extracellular ATP, leads to the aggregation and activation of the inflammasome, the multiprotein cytoplasmic complex required to activate caspase-1 and so initiate

caspase-1 proteolysis of pro-IL-1β into its bioactive 17kDa form (Martinon and Tschopp, 2004; Dinarello, 2005; Ferrari et al, 2006). In contrast, how the inflammasome is formed and activated in response to this secondary stimulus remains a puzzle. Most recently, at least two distinct inflammasome activation pathways subsequent to TLR signalling have been delineated (Mariathasan et al, 2004, 2006; Kanneganti et al, 2006; Martinon et al, 2006; Sutterwala et al, 2006): they are both associated with the adaptor protein ASC and involve caspase-1 cleavage but activation can be further distinguished by involvement of ICE-protease activating factor (IPAF), or by an IPAF-independent involvement of another adaptor protein, cryopyrin/NALP3/CIAS1. The latter, but not the former, pathway can be activated by P2X7R stimulation as well as Gram-positive but not Gram-negative bacteria (Mariathasan et al, 2004). While these recent studies have provided significant new insights into the composition of distinct inflammasomes and specificity of their activation, they have not addressed the underlying mechanisms of inflammasome activation. It has generally been accepted that P2X7R-mediated cleavage of caspase-1 is due to depletion of intracellular potassium resulting from ion flow through the small ion channel and/or the large dye-uptake pore (Gudipaty et al, 2003; Mariathasan et al, 2004; Dinarello, 2005; Ferrari et al, 2006). However, our results rule out intracellular K^+ depletion via P2X7R activation as the causative mechanism because panx1 inhibition abolished release of IL-1β without altering cellular K^+ depletion.

While detailed signalling mechanisms will require further elucidation, panx1 must now be considered the key upstream molecule in P2X7R-mediated inflammasome activation. It is tempting to speculate that panx-1 hemichannels, which can act as conduits for ATP release when overexpressed (Bao et al, 2004; Barbe et al, 2006; Locovei et al, 2006b), may subserve a similar role when natively activated by P2X7R

in macrophage. Concentrations of extracellular ATP (>100 μM) required to activate P2X7R may well be higher than free intracellular ATP concentrations, particularly as >90% of all intracellular ATP is produced in, and bound to, mitochondria (Tarasov et al, 2004). Because ATP can directly activate several caspases in cell-free assays (Han et al, 2003), and because elevations in intracellular ATP levels are associated with caspase activation and IL-1β release (Eguchi et al, 1997), the existence of a conduit for extracellular ATP entry into the cell would provide a novel mechanism for direct and immediate activation of caspase-1 processing by the inflammasome.

Materials and methods

Cells and reagents

CBX, phorbol 12-myristate 13-acetate (PMA), heptanol, mefloquine hydrochloride, ethidium bromide, ATP, gadolinium and Escherichia coli LPS were from Sigma, lanthanum from Fisher Bioscience, and YoPro1 from Invitrogen. THP-1 and J774 macrophage were cultured in RPMI, HeLa and 1321-N1 astrocytes in DMEM and HEK293 cells in F-12 media, all supplemented with 10% fetal calf serum (Gibco). Pure populations of human lung macrophage were isolated as described previously (Chong et al, 2003; Mackenzie et al, 2003).

Cloning, RT–PCR and qPCR

The full-length sequence encoding for human panx1 was amplified from PMA differentiated THP1 cDNA using PCR (Supplementary Figure 1A). c-myc (EQKLISEEDL), Glu-Glu (EYMPME) or eGFP tags were introduced in frame at the 30-end of the coding sequence using overlapping PCR and AccuzymeTM DNA polymerase (Bioline) before cloning into pcDNA3.1(-) vector (Invitrogen); hence, incorporating a c-myc, Glu-Glu (ee) or eGFP fusion tag at the C terminus of the expressed protein. Cloned products were confirmed by sequencing. Human brain RNA (Ambion) and total RNA from other cells were isolated using RNeasy Mini kit (Qiagen), followed by reverse transcription using SUPERSCRIPTTM III (Invitrogen) RNase H-reverse transcriptase with oligo-dT. Specific primers for panx1 (Supplementary Figure 1A), rat P2X7 (5'-TGGCAGTTCAGGGAGGAATC-3' and 5'-ACAGTTCCAAGAAGTCCG-3') or b-actin (5'-ATGGATGATGATATCGCCGCG-3' and 5'-CTAGAAGCATTTGCGGTG GAC-3') were used in PCR. The obtained product sizes for panx1 (610 bp), rat P2X7 (585 bp) and b-actin (1.1 kb) were as expected

from their mRNA sequences. Relative expression levels of panx1 and P2X7 mRNA were measured using an iCycler iQ real-time PCR detection system (BioRad) and iQ SYBR Green Supermix (BioRad). Specific primers for Panx-1 (Supplementary Figure 1A) and rat P2X7 (5'-TGTGCCTACAGGTGCTACGCC-3' and 5'-GCCCTTCACTCTTCGGAAACTC-3') were purchased from Sigma-Genosys, GAPDH specific primers from Qiagen (QuantiTech Primer Assays). For each primer set the efficiency was 495% and a single product was seen on melt curve analysis. Relative expression levels were calculated using the $2^{-\Delta\Delta Ct}$ method normalizing to GAPDH expression levels (Livak and Schmittgen, 2001).

siRNA and peptides

Small interference RNAs against human panx1 were SilencerTM (Ambion) predesigned (Supplementary Figure 1A). siRNA (200 pmol) transfection was with Lipofectamine 2000 (Invitrogen), experiments were carried out 2 days posttransfection. The panx1 mimetic blocking peptide 10panx1 (WRQAAFVDSY), the connexin 32 blocking peptide gp27 (SRPTEKTVFT) and other peptides (Supplementary Figure 1β) were synthesized by Sigma-Genosys and Alta Biosciences.

Electrophysiology and fluorescence assays

Details are as described previously (Mackenzie et al, 2001; Jiang et al, 2005). Simultaneous whole-cell patch clamp recordings, capacitance tracking and YoPro1 or ethidium fluorescence were carried out under Fluar x40 objective on a Zeiss Axiovert 100 using EPC9 amplifier (HEKA) and Photonics monochromator imaging system.

Other dye uptake and Fluo4 calcium imaging experiments were carried out using a Nikon confocal microscope under x20 or x40 objective; 20–60 isolated (not touching) cells were imaged in each experiment, averaged, and the slope of the fluorescence signal was used as the most accurate and consistent measurement for comparisons. Measurements of fluorescence intensity (fluorescence units, f.u.) at 100s after compound application gave similar results but showed greater inter-experiment variability. All protocols and extracellular solutions were the same under both systems: YoPro1 (2μM) or ethidium bromide (20μM) was present throughout unless otherwise stated; because YoPro1 and GFP fluorescence overlap, ethidium (red spectrum) was used in all experiments involving transient transfections as we used eGFP co-transfection to identify transfected cells. Digitonin (100μM) was used at the end of the experiments to induce maximum dye uptake. Except where stated otherwise, external solution was (mM) NaCl 147, HEPES 10, glucose 13, $CaCl_2$ 2, $MgCl_2$ 1 and KCl 2; internal solution was NaCl 147 or Cs-gluconate, HEPES 10, EGTA 10 and $MgCl_2$ 3. All recordings were performed only on single, isolated cells in order to preclude effects due to gap junctions.

Co-immunoprecipitation, Western blotting and immunohistochemistry

HEK cells stably expressing P2X7-ee tagged receptor were transfected with panx1 c-myc cDNA or empty pcDNA3.1 (used as negative controls for anti-c-myc co-immunoprecipitations) and lysed in RIPA buffer (20 mM Tris–HCl pH 7.4, 150 mM NaCl, 1mM $MgCl_2$, 1mM $CaCl_2$, 1% Triton X-100) supplemented with Complete protease inhibitor cocktail (Roche). Lysates were centrifuged to remove particulate matter, resolved in 4–10% polyacrylamide gels and transferred onto PVDF membranes (Millipore) by electro-blotting. For immunoprecipitations, lysates were pre-

cleaned with protein G sepharose beads (Amersham Biosciences) before immunoprecipitation with mouse anti-c-myc (Covance) or control mouse IgG (Vector) and immunoblotted with rabbit anti-ee (Bethyl) or rabbit anti-c-myc (Covance). Immunohistochemistry was carried out using rabbit anti-ee Ab and photographed under the Nikon confocal microscope.

IL-1β release and K^+ release

J774 macrophages, human lung macrophages or PMA differentiated THP-1 macrophage were stimulated with LPS (0.1–1 μg/ml) for 4h (Mackenzie et al, 2001; Kahlenberg and Dubyak, 2004), washed and preincubated for 30 min with 1 mg/ml of anti-P2X7 antibody (Buell et al, 1998), 50 μM CBX, 100 μM of cell-permeable and irreversible inhibitor of caspase-1 (Ac-YVAD-2,6-dimethylben-zoyloxymethyl ketone (AOM), caspase-1 inhibitor IV, Calbiochem) or 500 μM of 10panx1 or 1mM gp27 peptide and ATP applied for 30 min. Supernatants were assayed for IL-1β by ELISA (Mackenzie et al, 2001) using anti-human IL-1β (Endogen) as the coating antibody, anti-human IL-1β-biotin (Pierce) as the detection antibody for THP-1 and for human lung macrophage. J774 supernatants were assayed using Quantikines mouse IL-1β kit (R&D Systems) following the manufacturer instructions. For Western blot analysis, macrophage cell extracts were prepared as detailed above and supernatants were concentrated using 10-kDa nominal molecular weight cutoff filters (Millipore) and immunobloted with anti-IL-1β antibody (3ZD, provided by the Biological Resources Branch of the National Cancer Institute, Frederick Cancer Research and Development Centre, Frederik, MD) or with anti-caspase-1 p10 rabbit polyclonal antibody for mouse (Santa Cruz). Cellular and released Kþ were measured against standards using the Ciros Vision inductively coupled plasma-atomic emission spectrometer (Spectro

Analytical UK Ltd). For these experiments, cells were lysed in 1ml of 10% nitric acid with parallel wells used for IL-1β assays.

Statistical analysis

Average results are expressed as the mean±s.e.m. from the number of assays indicated. Data were analyzed by an unpaired Student's t-test to determine difference between groups using Instat (Graph-Pad) and Excel (Microsoft) software.

Acknowledgements

We thank L Collinson and E Martin for molecular biology and tissue culture support. We are indebted to Dr P Peachell, Royal Hallamshire Hospital, University of Sheffield for invaluable help in providing human lung preparations. The Centre for Chemical Instrumental Analysis and Services, Department of Chemistry, University of Sheffield, analysed K^+ content of our samples. This work supported by the Wellcome Trust and a postdoctoral fellowship to PP from AstraZeneca Charnwood.

Competing interests statement

The authors state that they have no competing financial interests.

References

Bao L, Locovei S, Dahl G (2004) Pannexin membrane channels are mechanosensitive conduits for ATP. FEBS Lett 572: 65–68

Barbe MT, Monyer H, Bruzzone R (2006) Cell–cell communication beyond connexins: the pannexin channels. Physiology 21: 103–114

Beyer EC, Steinberg TH (1991) Evidence that the gap junction protein connexin-43 is the ATP-induced pore of mouse macrophages. J Biol Chem 266: 7971–7974

Bruzzone R, Barbe MT, Jakob NJ, Monyer H (2005) Pharmacological properties of homomeric and heteromeric pannexin hemichannels expressed in Xenopus oocytes. J Neurochem 92: 1033–1043

Buell G, Chessell IP, Michel AD, Collo G, Salazzo M, Herren S, Gretener D, Grahames C, Kaur R, Kosco-Vilbois MH, Humphrey PP (1998) Blockade of human P2X7 receptor function with a monoclonal antibody. Blood 92: 3521–3528

Chong LK, Suvarna K, Chess-Williams R, Peachell PT (2003) Desensitization of b2-adrenoceptor-mediated responses by short-acting b2-adrenoceptor agonists in human lung mast cells. Br J Pharmacol 138: 512–520

Dhein S (2004) Pharmacology of gap junctions in the cardiovascular system. Cardiovasc Res 62: 287–298

Dinarello CA (2005) Blocking IL-1 in systemic inflammation. J Exp Med 201: 1355–1399

Eguchi Y, Shimizu S, Tsujimoto Y (1997) Intracellular ATP levels determine cell death fate by apoptosis or necrosis. Cancer Res 57: 1835–1840

Elliott JI, Surprenant A, Marelli-Berg FM, Cooper JC, Cassady-Cain RL, Wooding C, Linton K, Alexander DR, Higgins CF (2005) Membrane phosphatidylserine distribution as a non-apoptotic signalling mechanism in lymphocytes. Nat Cell Biol 7: 808–816

Faria RX, Defarias FP, Alves LA (2005) Are second messengers crucial for opening the pore associated with P2X7 receptor? Am J Physiol 288: C260–C270

Ferrari D, Pizzirani C, Adinolfi E, Lemoli RM, Curti A, Idzko M, Panther E, Di Virgilio F (2006) The P2X7 receptor: a key play in IL-1 processing and release. J Immunol 176: 3877–3883

Griffith TM, Chaytor AT, Edwards DH (2004) The obligatory link: role of gap junctional communication in endothelial dependent smooth muscle hyperpolarization. Pharmacol Res 49: 551–564

Gudipaty L, Munetz J, Verhoef PA, Dubyak GR (2003) Essential role for Ca2+ in regulation of IL-1βeta secretion by P2X7 nucleotide receptor in monocytes, macrophages and HEK-293 cells. Am J Physiol 285: C286–C299

Han BS, Hong HS, Choi WS, Markelonis GJ, Oh TH, Oh YJ (2003) Caspase-dependent and independent cell death pathways in primary cultures of mesencephalic dopaminergic neurons after neurotoxin treatment. J Neurosci 23: 5069–5078

Hickman SE, Semrad CE, Silverstein SC (1996) P2Z purinoceptors. Ciba Found Symp 198: 71–83

Humphreys BD, Dubyak GR (1998) Modulation of P2X7 nucleotide receptor expression by pro- and anti-inflammatory stimuli in THP-1 monocytes. J Leukoc Biol 64: 265–273

Jiang LH, Rassendren F, Mackenzie A, Zhang YH, Surprenant A, North RA (2005) N-methyl-D-glucamine and propidium dyes utilize different permeation pathways at rat P2X7 receptors. Am J Physiol 289: C1295–C1302

Kahlenberg JM, Dubyak GR (2004) Mechanisms of caspase-1 activation by P2X7 receptor-mediated K+ release. Am J Physiol 286: C1100–C1108

Kanneganti TD, Ozoren N, Body-Malapel M, Amer A, Park JH, Franchi L, Whitfield J, Barchet W, Colonna M, Vandenabeele P, Bertin J, Coyle A, Grant EP, Akira S, Nunez G (2006) Bacterial RNA and small antiviral compounds activate caspase-1 through cryopyrine/Nalp3. Nature 440: 233–236

Ke HZ, Qi H, Weidema AF, Zhang Q, Panupinthu N, Crawford DT, Grasser WA, Paralkar VM, Li M, Audoly LP, Gabel CA, Jee WS, Dixon SJ, Sims SM, Thompson DD (2003) Deletion of the P2X7 nucleotide receptor reveals its regulatory roles in bone formation and resorption. Mol Endocrinol 17: 1356–1367

Livak KJ, Schmittgen TD (2001) Analysis of relative gene expression data using real-time quantitative PCR and the 2(-ΔΔC(T)) method. Methods 25: 402–408

Locovei S, Bao L, Dahl G (2006a) Pannexin 1 in erythrocytes: function without a gap. Proc Natl Acad Sci 103: 7655–7659

Locovei S, Wang J, Dahl G (2006b) Activation of pannexin 1 channels by ATP through P2Y receptors and by cytoplasmic calcium. FEBS Lett 580: 239–244

Mackenzie A, Wilson HL, Kiss-Toth E, Dower SK, North RA, Surprenant A (2001) Rapid secretion of interleukin 1β by microvesicle shedding. Immunity 8: 825–835

Mackenzie AB, Chirakkal H, North RA (2003) Kv1.3 potassium channels in human alveolar macrophage. Am J Physiol 285: L862–L868

Mackenzie AB, Young MT, Adinolfi E, Surprenant A (2005) Pseudoapoptosis induced by brief activation of ATP-gated P2X7 receptors. J Biol Chem 280: 33968–33976

Mariathasan S, Newton K, Monack DM, Vucic D, French DM, Lee WP, Roose-Girma M, Erickson S, Dixit VM (2004) Differential activation of the inflammasome by caspase-1 adaptors ASC and Ipaf. Nature 430: 213–218

Mariathasan S, Weiss DS, Newton K, McBride J, O'Rourke K, Roose-Girma M, Lee WP, Weinrauch Y, Monack DM, Dixit VM (2006) Cryopyrin activates the inflammasome in response to toxins and ATP. Nature 440: 228–232

Martinon F, Tschopp J (2004) Inflammatory caspases: linking an intracellular innate immune system to autoinflammatory diseases. Cell 117: 561–574

Martinon F, Petrilli V, Mayor A, Tardivel A, Tschopp J (2006) Gout-associated uric acid crystals activate the NALP3 inflammasome. Nature 440: 237–241

Morelli A, Chiozzi P, Chiesa A, Ferrari D, Sanz JM, Falzoni S, Pinton P, Rizzuto R, Olson MF, Di Virgilio F (2003) Extracellular ATP causes ROCK I-dependent bleb formation in P2X7-transfected HEK cells. Mol Biol Cell 14: 2655–2664

Nemeth K, Bugovics G, Skekely J (1997) Antiapoptotic effect of benzyloxycarbonyl-aspartyl-(b-tertier-butyl ester)-bromomethyl-ketone (Z-D(OtBu)-BMK), an intermediate of interleukin-1β converting enzyme inhibitors. Int J Immunopharmacol 19: 215–225

North RA (2002) Molecular physiology of P2X receptors. Physiol Rev 82: 1013–1067

Panchin YV (2005) Evolution of gap junction proteins—the pannexin alternative. J Exp Biol 208: 1415–1419

Perregaux D, Gabel CA (1994) Interleukin-1 beta maturation and release in response to ATP and nigericin. Evidence that potassium depletion mediated by these agents is a necesary and common feature of their activity. J Biol Chem 269: 15195–15203

Perregaux DG, Svensson L, Gabel CA (1996) Tenidap and other anion transport inhibitors disrupt cytolytic T lymphocyte- mediated IL-1 beta post-translational processing. J Immunol 157: 57–64

Schilling WP, Wasylyna T, Dubyak GR, Humphreys BD, Sinkins WG (1999) Maitotoxin and P2Z/P2X7 purinergic receptor stimulation activate a common cytolytic pore. Am J Physiol 277: C766–C776

Solle M, Labasi J, Perregaux DG, Stam E, Petrushova N, Koller BH, Griffiths RJ, Gabel CA (2001) Altered cytokine production in mice lacking P2X7 receptors. J Biol Chem 276: 125–132

Spray DC, Rozental R, Srinivas M (2002) Prospects for rational development of pharmacological gap junction channel blockers. Curr Drug Targets 3: 455–464

Steinberg TH, Di Virgilio F (1991) Cell-mediated cytotoxicity: ATP as an effector and the role of target cells. Curr Opin Immmunol 3: 71–75

Suadicani SO, Brosnan CF, Scemes E (2006) P2X7 receptors mediate ATP release and amplification of astrocytic intracellular Ca2+ signaling. J Neurosci 26: 1378–1385

Sutterwala FS, Ogura Y, Szczepanik M, Lara-Tejero M, Lichtenberger GS, Grant EP, Bertin J, Coyle AJ, Galan JE, Askenase PW, Flavell RA (2006) Critical role for NALP3/CIAS1/ cryopyrin in innate and adaptive immunity through its regulation of caspase-1. Immunity 24: 317–327

Tarasov A, Dusonchet J, Ashcroft F (2004) Metabolic regulation of the pancreatic b-cell ATP-sensitive K+ channel. Diabetes 53: S113–S122

Thompson RJ, Zhou N, MacVicar BA (2006) Ischemia opens neuronal gap junction hemichannels. Science 312: 924–927

Figure Legends

Figure 1. Panx1 is associated with P2X7R protein and its signalling. (A) Panx1 mRNA detected by RT–PCR from human and mouse cells as indicated; THP-1 macrophages, lung alveolar macrophage, Jurkat lymphocytes and mouse J774 macrophage show highest expression. (B) RT–PCR example and qPCR summary showing panx1 mRNA upregulation by PMA (0.5 μM for 30 min) and further increased by PMA plus LPS (100 ng/ml for 4 h). (C) HEK cells stably expressing P2X7-ee receptor were transfected with Panx1-myc and immunoprecipitation (IP) of cell lysates with anti-myc Ab carried out followed by Western blotting (WB) with anti-ee Ab. (D) Immunohistochemical localization of panx1 (red) to plasma membrane in HEK cell co-transfected with panx1-ee and eGFP (green, cytoplasmic localization, left-hand panel); photo on right is HEK P2X7-expressing cell transfected with panx1-eGFP construct showing panx1 protein in blebs induced by ATP stimulation. (E, F) siRNA knockdown of endogenous levels of panx1 mRNA in HEK cells (E) and exogenously expressed panx1 protein (F). mRNA levels show mean7s.e.m. from qPCR assays for four separate experiments, $P<0.001$ for panx1 mRNA levels of cells transfected with siRNA70 versus scrambled siRNA. For WB, lysates were immunoblotted with anti-ee (panx1), anti-P2X7R and anti-b-actin as loading control; note panx1 siRNA did not alter levels of P2X7R.

Figure 2. Selective inhibition of Panx1 blocks P2X7R-induced dye uptake but not ionic currents. (A) Representative traces of simultaneous recording of membrane current and ethidium uptake from control or panx1 siRNA70 transfected HEK cell expressing P2X7R in response to 3mM ATP stimulation. (B) Similar recordings obtained from control cell and cell exposed to 10panx1 peptide (200μM for 10min). (C)

Representative photos (5min in ATP) and kinetic traces of ethidium uptake recorded from populations of P2X7R expressing or non-expressing HEK cells as indicated after transfection with scrambled or panx1 siRNA70. Digitonin (100 μM) applied at end of experiment to induce maximum dye uptake; siRNA did not alter ethidium fluorescence after digitonin treatment (n=20 cells for each treatment and representative of 7 independent experiments). (D) Summary of all dye uptake obtained from siRNA experiments illustrated in A and C. Histograms show slope of dye uptake in response to maximum concentration of ATP (5 mM) from cells transfected with scrambled (control) or panx1-targettted siRNA; siRNA70 reduced ATP-evoked dye uptake by >80%. **P<0.001. (E) Kinetic traces of ethidium uptake from mouse J774 or human alveolar macrophage in the absence or presence of 10panx1-mimetic peptide (100 μM for 20 min); each trace is mean±s.e.m. of 50 cells in field of view and representative of 2–6 independent experiments. (F) Plots EC50 concentration of ATP, maximum current amplitude and dye uptake induced by maximum ATP concentration (expressed as % control response) from P2X7R-expressing HEK cells transfected with panx1 siRNA70, and from HEK, J774 and human alveolar macrophage incubated for 10–30 min with 10panx1 peptide as indicated. In all cases dye-uptake was reduced by >80% without alteration of membrane currents.

Figure 3. Overexpression of panx1 induces constitutive dye-uptake and hemichannel-like currents selectively blocked by 10panx1 and CBX. (A) Ethidium uptake in P2X7R-negative HEK cells transfected with empty or panx1 expression vector; superfusion of cells with ethidium resulted in immediate uptake in panx1 transfected cells; each trace is mean±s.e.m. of 50 cells in field of view. (B) Similar experiment in P2X7R-positive HEK cells; ethidium application did not result in

constitutive dye uptake but the ATP-evoked response showed faster kinetics and maximum fluorescence; traces are mean±s.e.m. of 50 cells. Western blots obtained from cells used in these experiments are shown; panx1 overexpression did not change P2X7R protein expression. (C) Currents in response to ramp voltages (–120 to 80mV) from control (GFP- transfected) or panx1 transfected HEK cell in normal extracellular solution, in solution containing the larger cation NMDG in place of sodium, in the presence of lanthanum (100 μM), gadolinium (100 μM) or CBX (5 μM) as indicated. (D) Currents from panx1 transfected HEK cell in 0 (control), 5 and 12 min in presence of 100 μM 10panx1 peptide and 15 min after washout; complete inhibition was observed within 10–15 min. (E) Summary of all similar experiments where current at 60 mV is shown as % of control response; only 10panx1 peptide and CBX (20 μM) inhibited the current while other connexin hemichannel inhibitors (heptanol, gp27 peptide and replacing sodium with calcium) or Trp channel inhibitors (NMDG, lanthanum, gadolinium) were without effect. Removal of extracellular calcium, which activates connexin hemichannel currents, also was without effect on panx1 currents (n = 24 for CBX and lanthanum, nine for 10panx1 peptide and six for others).

Figure 4. CBX but not other connexin channel blockers blocks ATP-mediated dye-uptake without inhibiting P2X7R activation. (A, B) Membrane currents, YOPRO-1 uptake and Fluo4 calcium transients (as indicated) recorded from HEK (A) or 1321-N1 (B) cells expressing P2X7Rs. CBX (20μM) effectively blocked YOPRO-1 uptake without altering currents or calcium transients. All recordings obtained from physically isolated, single cells. (C) ATP concentration–response curves for membrane current (recorded at –60 mV holding potential) from all experiments as

illustrated in (A) and (B), in control (closed symbols) and in 20 μM CBX (open symbols) for HEK cells expressing rat or human P2X7R, for 1321-N1 cells expressing human P2X7R and for mouse J774 macrophage, as indicated. CBX had no effect. (D) Concentration–response curve for CBX inhibition of dye uptake (circles) in P2X7R-expressing cells and for inhibition of panx1 currents recorded from HEK cells (squares) transfected with panx1 expression vector. (E) Summary of actions of several nonspecific connexin channel blockers to inhibit P2X7R-induced dye uptake from cells ectopically (HEK and 1321-N1) or endogenously (mouse J774 and human alveolar macrophage) expressing P2X7R. Concentrations used were CBX (20 μM), heptanol (200 μM), mefloquine (100 μM) and gp27 (1 mM); each value is mean±s.e.m. from 4 to 12 experiments.

Figure 5. Panx1 blockade inhibits ATP-mediated IL-1β release from activated macrophage. (A) IL-1β release from LPS-primed THP-1 macrophages after transfection with scrambled or panx1 siRNA70. Neither siRNA alone induced IL-1β release nor did the scrambled siRNA alter ATP-induced release relative to untransfected cells, but panx1 siRNA70 significantly inhibited ATP-induced release; results are representative of three similar experiments. **P<0.005. (B) IL-1β release from LPS-primed THP-1 macrophages under conditions indicated. CBX (20 μM), 10pan1 peptide (200 μM) and the monoclonal anti-P2X7R Ab, but not the connexin blocking peptide gp27 (1 mM), significantly inhibited ATP-evoked IL-1β release. (C, D) Similar experiments performed on mouse J774 macrophage and human alveolar macrophage; 10panx1 inhibitory peptide completely blocked ATP-mediated IL-1β

release from these cells. Results are representative of 3–6 similar experiments in each case; error bars are standard deviation of triplicate samples. **P<0.005.

Figure 6. Panx1 blockade inhibits IL-1β processing but not intracellular K^+ depletion from LPS-primed macrophage. Western blot analysis of cell lysate and medium from human THP-1 macrophages (A), mouse J774 macrophage (B) and human alveolar macrophage (C). No 17 kDa form was present intracellularly under any condition, while medium contained both pro-IL-1β and fully processed, 17 kDa, IL-1β only after LPS priming and ATP treatment. No processed 17kDa IL-1β was observed in the medium after treatment with 10panx1 inhibitory peptide. (D) Intracellular and released K^+ (plotted as fraction of control) from parallel wells of J774 cells treated as in (B), n = 4.

Figure 7. Panx1 inhibition blocks intracellular caspase 1 processing. Western blot analysis of mouse J774 macrophage for caspase-1 (A) and IL-1β (B). (A) Same gel is shown, upper lanes with short exposure and lower lanes with longer exposure; we used short exposure to assess p45 pro-caspase-1 protein levels in each lane and longer exposure to reveal processing and active caspase-1 p10 fragment. After LPS priming, ATP induced strong caspase-1 processing, which was prevented by either 10panx1 inhibitory peptide or the caspase-1 inhibitor, Ac-YVAD-AOM. (B) Western blot for IL-1β from same set of experiments confirms ATP-mediated IL-1β processing and release are also prevented by 10panx1 inhibitory peptide or caspase-1 inhibitor.

Figure 1

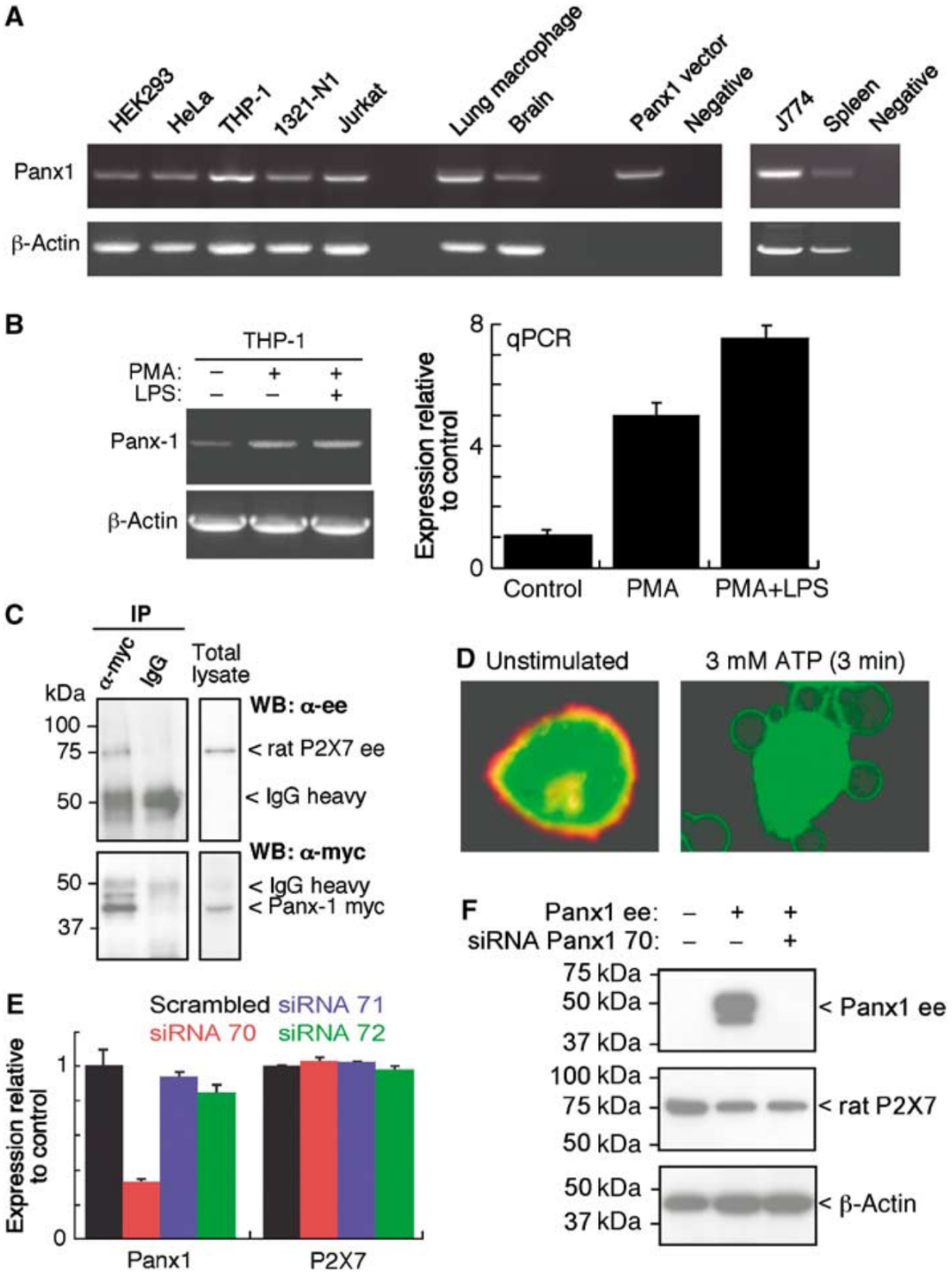
A
HEK293
HeLa
THP-1
1321-N1
Jurkat
Lung macrophage
Brain
Panx1 vector
Negative
J774
Spleen
Negative
Panx1
β-Actin
B
THP-1
PMA: – + +
LPS: – – +
Panx-1
β-Actin
qPCR
Expression relative to control
8
4
0
Control
PMA
PMA+LPS
C
IP
α-myc
IgG
Total lysate
kDa
100
75
50
WB: α-ee
< rat P2X7 ee
< IgG heavy
WB: α-myc
50
37
< IgG heavy
< Panx-1 myc
D Unstimulated
3 mM ATP (3 min)
E
Scrambled siRNA 71
siRNA 70 siRNA 72
Expression relative to control
1
0
Panx1
P2X7
F
Panx1 ee: – + +
siRNA Panx1 70: – – +
75 kDa
50 kDa
37 kDa
< Panx1 ee
100 kDa
75 kDa
50 kDa
< rat P2X7
50 kDa
37 kDa
< β-Actin

Figure 2

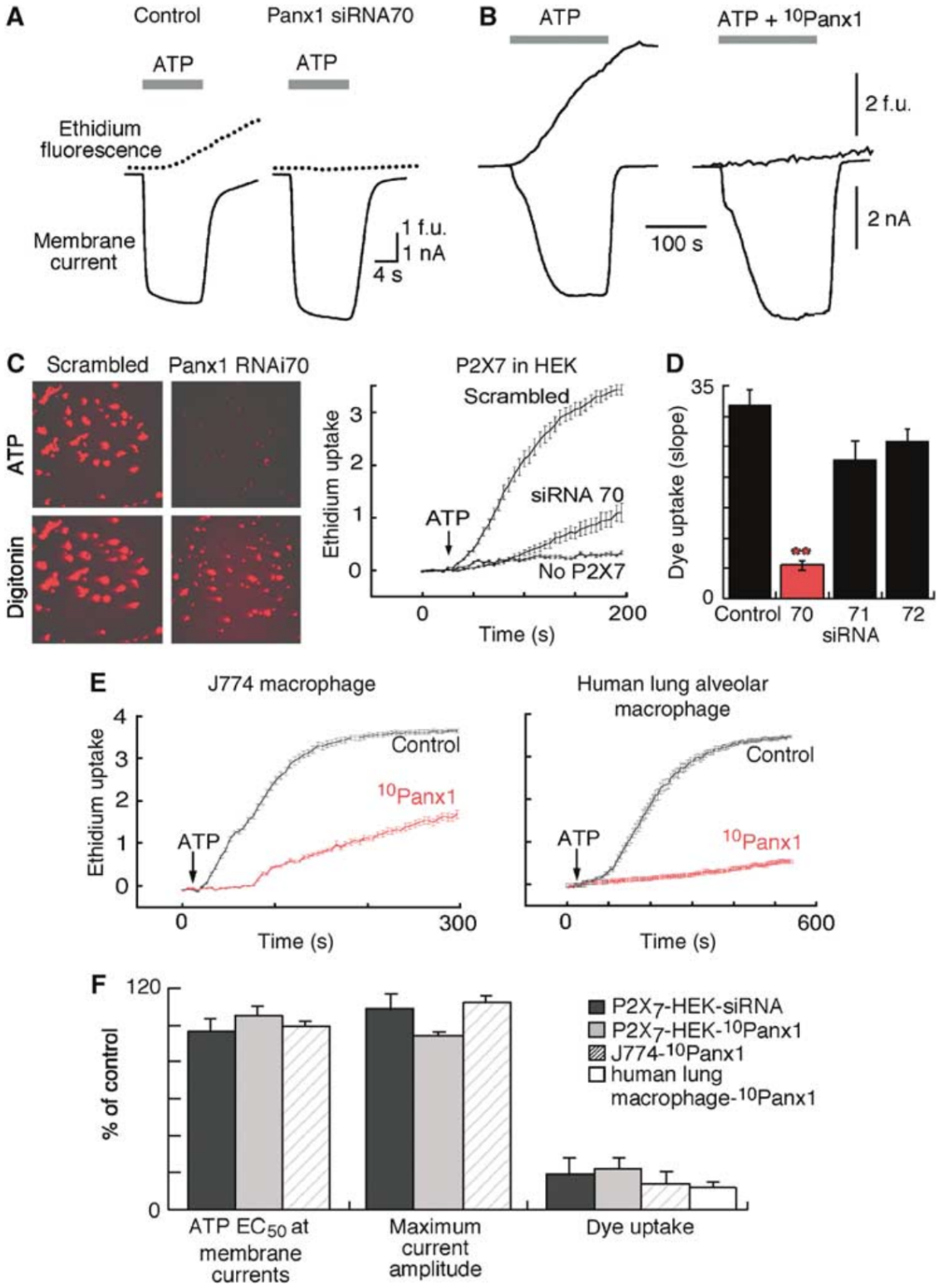
A
Control
Panx1 siRNA70
ATP
ATP
Ethidium fluorescence
Membrane current
1 f.u.
1 nA
4 s
B
ATP
ATP + 10Panx1
2 f.u.
2 nA
100 s
C
Scrambled
Panx1 RNAi70
ATP
Digitonin
P2X7 in HEK
Scrambled
siRNA 70
No P2X7
ATP
Ethidium uptake
Time (s)
D
Dye uptake (slope)
Control
70
71
72
siRNA
E
J774 macrophage
Human lung alveolar macrophage
Control
10Panx1
ATP
Ethidium uptake
Time (s)
F
% of control
P2X7-HEK-siRNA
P2X7-HEK-10Panx1
J774-10Panx1
human lung macrophage-10Panx1
ATP EC50 at membrane currents
Maximum current amplitude
Dye uptake

Figure 3

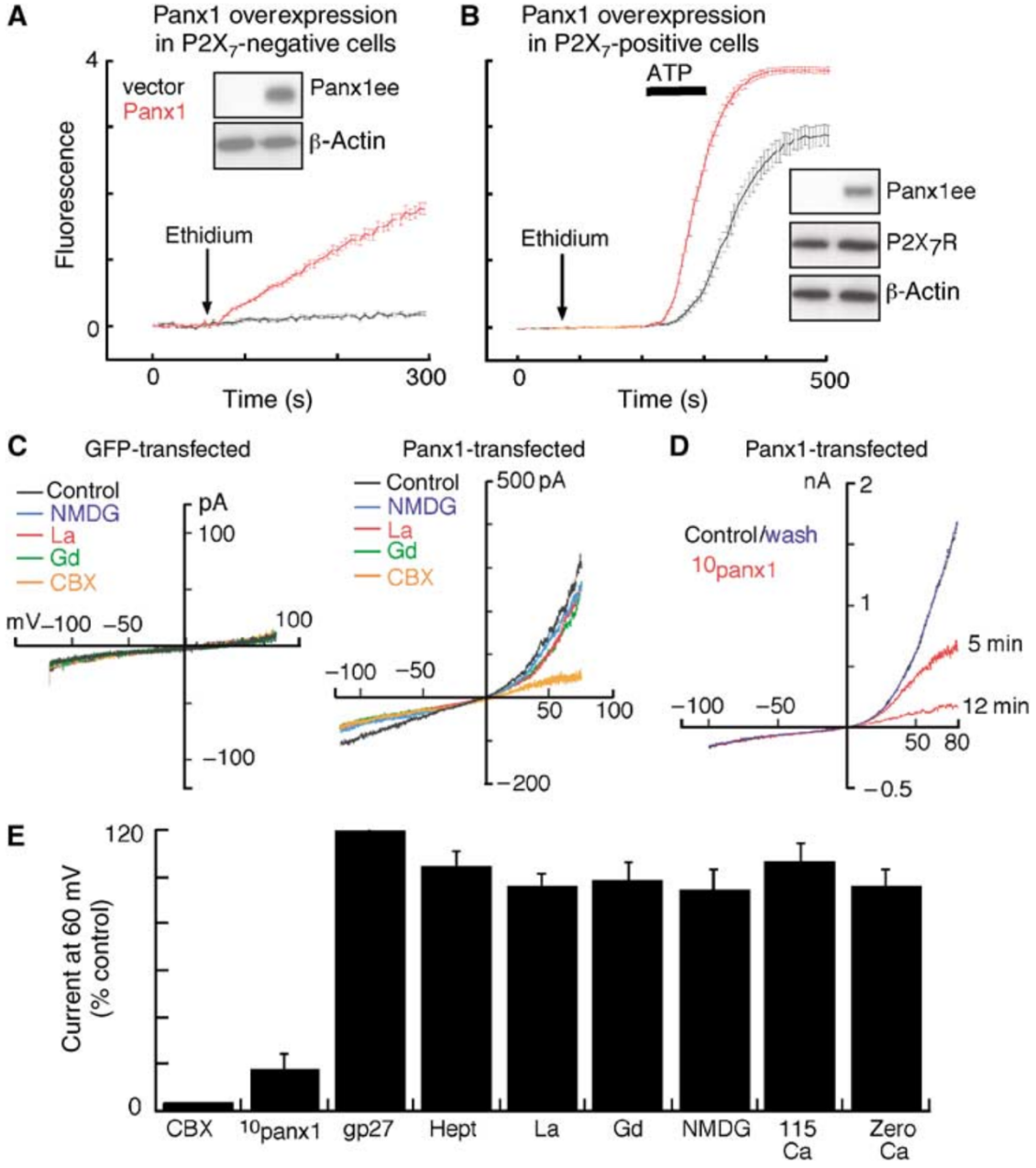
A
Panx1 overexpression
in P2X7-negative cells
vector
Panx1
Panx1ee
β-Actin
Ethidium
Fluorescence
4
0
0
300
Time (s)
B
Panx1 overexpression
in P2X7-positive cells
ATP
Ethidium
Panx1ee
P2X7R
β-Actin
0
500
Time (s)
C
GFP-transfected
Control
NMDG
La
Gd
CBX
pA
100
mV −100 −50
100
−100
Panx1-transfected
Control
NMDG
La
Gd
CBX
500 pA
−100 −50
50 100
−200
D
Panx1-transfected
nA
2
Control/wash
10panx1
1
5 min
12 min
−100 −50
50 80
−0.5
E
Current at 60 mV
(% control)
120
0
CBX
10panx1
gp27
Hept
La
Gd
NMDG
115 Ca
Zero Ca

Figure 4

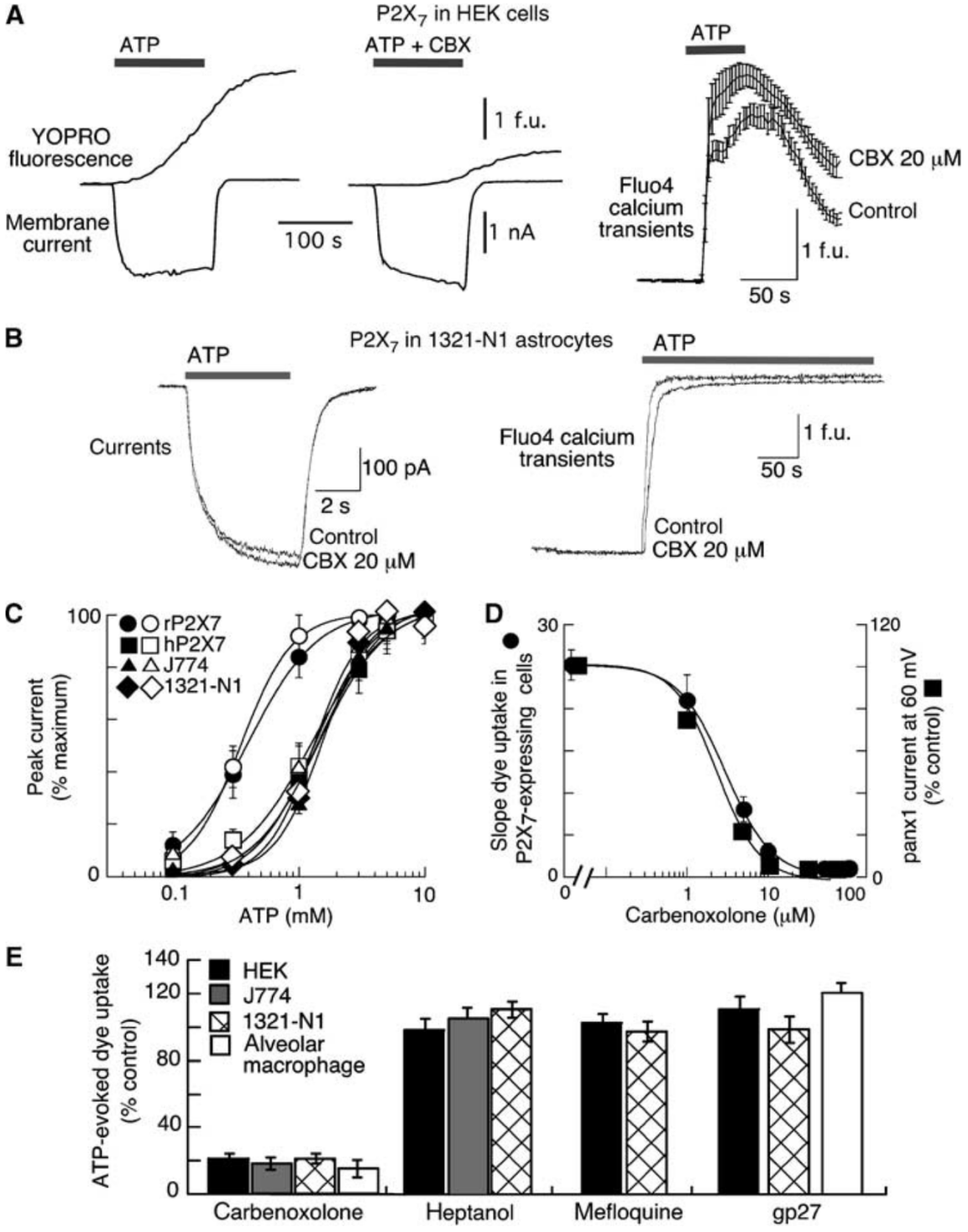
A
P2X7 in HEK cells
ATP
ATP + CBX
YOPRO fluorescence
Membrane current
100 s
1 f.u.
1 nA
ATP
Fluo4 calcium transients
CBX 20 μM
Control
1 f.u.
50 s
B
P2X7 in 1321-N1 astrocytes
ATP
Currents
100 pA
2 s
Control
CBX 20 μM
ATP
Fluo4 calcium transients
1 f.u.
50 s
Control
CBX 20 μM
C
rP2X7
hP2X7
J774
1321-N1
Peak current (% maximum)
100
0
0.1
1
10
ATP (mM)
D
Slope dye uptake in P2X7-expressing cells
panx1 current at 60 mV (% control)
30
0
120
0
0
1
10
100
Carbenoxolone (μM)
E
ATP-evoked dye uptake (% control)
140
120
80
40
0
HEK
J774
1321-N1
Alveolar macrophage
Carbenoxolone
Heptanol
Mefloquine
gp27

Figure 5

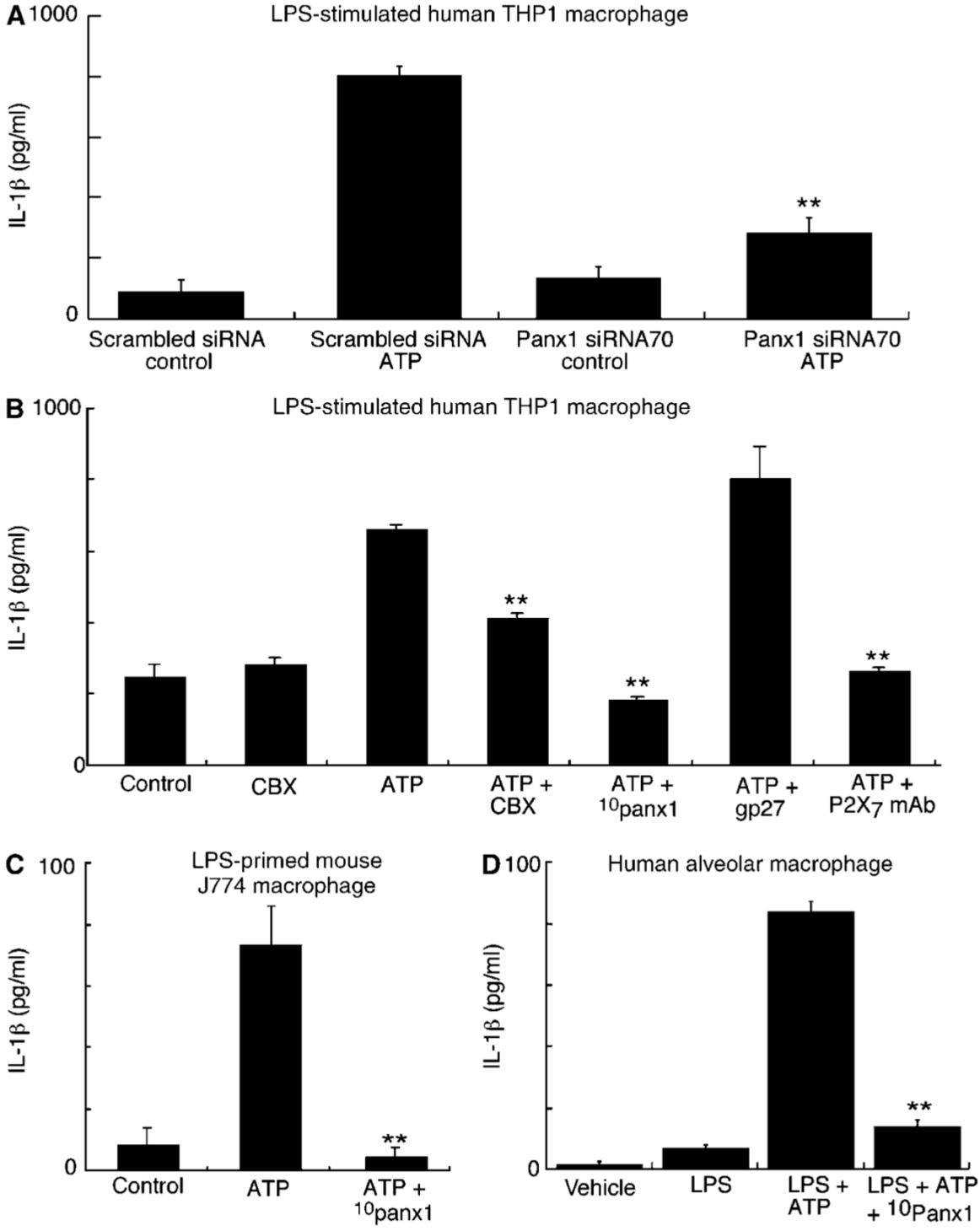
A
1000
LPS-stimulated human THP1 macrophage
IL-1β (pg/ml)
0
**
Scrambled siRNA control
Scrambled siRNA ATP
Panx1 siRNA70 control
Panx1 siRNA70 ATP
B
1000
LPS-stimulated human THP1 macrophage
IL-1β (pg/ml)
0
**
**
**
Control
CBX
ATP
ATP + CBX
ATP + 10panx1
ATP + gp27
ATP + P2X7 mAb
C
100
LPS-primed mouse J774 macrophage
IL-1β (pg/ml)
0
**
Control
ATP
ATP + 10panx1
D
100
Human alveolar macrophage
IL-1β (pg/ml)
0
**
Vehicle
LPS
LPS + ATP
LPS + ATP + 10Panx1

Figure 6

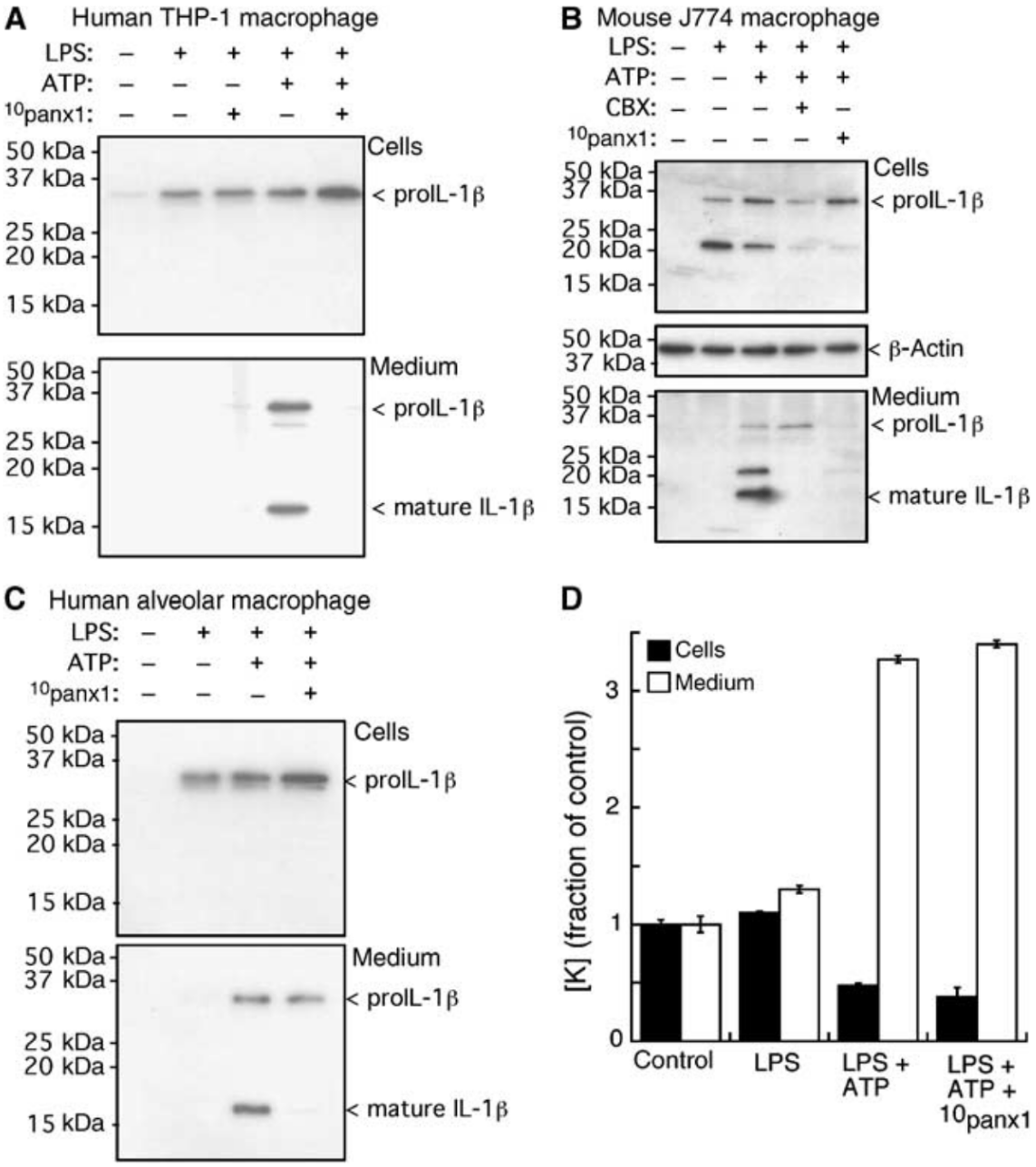
A
Human THP-1 macrophage
LPS: – + + + +
ATP: – – – + +
10panx1: – – + – +
50 kDa
37 kDa
25 kDa
20 kDa
15 kDa
Cells
< proIL-1β
Medium
< proIL-1β
< mature IL-1β
B
Mouse J774 macrophage
LPS: – + + + +
ATP: – – + + +
CBX: – – – + –
10panx1: – – – – +
< β-Actin
C
Human alveolar macrophage
LPS: – + + +
ATP: – – + +
10panx1: – – – +
D
Cells
Medium
[K] (fraction of control)
0
1
2
3
Control
LPS
LPS + ATP
LPS + ATP + 10panx1

Figure 7

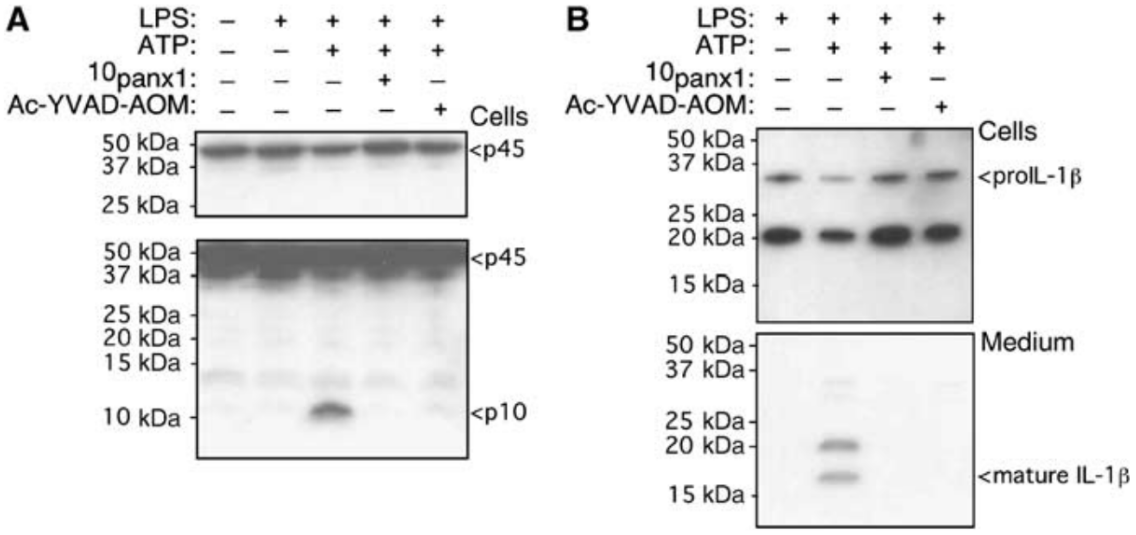
A
LPS: – + + + +
ATP: – – + + +
10panx1: – – – + –
Ac-YVAD-AOM: – – – – +
Cells
50 kDa
37 kDa
25 kDa
<p45
50 kDa
37 kDa
25 kDa
20 kDa
15 kDa
10 kDa
<p45
<p10
B
LPS: + + + +
ATP: – + + +
10panx1: – – + –
Ac-YVAD-AOM: – – – +
Cells
50 kDa
37 kDa
25 kDa
20 kDa
15 kDa
<prolL-1β
Medium
50 kDa
37 kDa
25 kDa
20 kDa
15 kDa
<mature IL-1β

Supplementary Figure 1 Cloning, RT-PCR, qPCR and generation of pannexin siRNA and blocking peptides. (A) coding sequence of human Panx1, binding sites for oligonucleotides used to amplify and clone panx1 are shown in orange, for oligonucleotides used in RT-PCR in green and specific forward oligonucleotide used for qPCR is boxed (this was used together with reversed oligonucleotide used for RT-PCR). The different siRNA target sites are highlighted in blue. (B) Schematic of panx1 protein indicating residues used to generate the ^{10}panx1 blocking peptide and one of the negative peptides, ^{14}panx1. ^{10}Panx1 and gp27 residues (used in the present study as a selective connexin channel inhibitor as well as a negative control peptide) are conserved in mouse, rat and human proteins. (C) Example of lack of effect of one of the panx1-mimetic peptides, ^{14}panx1 peptide, on ATP-evoked dye uptake assayed on HEK-P2X$_7$ expressing cells (traces representative of 4 independent experiments). We generated a total of 8 different panx1-mimetic peptides (ranging from 8 to 21 residues) but only ^{10}panx1-mimetic peptide had an effect on P2X$_7$R-induced dye uptake.

Supplementary Figure 2 Pharmacological characterization of panx1-mimetic peptide (A) and LDH release measured from all IL-1β release experiments (B). (A) Concentration-inhibition curves for panx1-mimetic inhibitory peptide, ^{10}panx1, on overexpressed panx1 HEK cells, current measured at 60 mV (circles, n = 7 for each point) and for ATP-evoked dye-uptake from P2X$_7$R-expressing HEK cells (squares, n = 4 experiments, 20-30 cells in field of view averaged for each experiment). IC$_{50}$ values for inhibition of panx1 currents and ATP-evoked dye uptake were not significantly different (52 ± 12 μM and 93 ± 21 μM, respectively). (B) Graphs show LDH release (% total intracellular LDH) for all conditions used in the present study. LDH levels were measured from each individual experiment described in this study and are shown here as mean ± sem; error bars are within the limits of the symbols in each case.

Supplementary Fig. 1

A

```
ATGGCCATCGCTCAACTGGCCACGGAGTACGTGTTCTCGGATTTCTTGCTGAAGGAGCCCACGGAGCCCAAGTTCAAGGGGCTGCGACT
GGAGCTGGCTGTGGACAAGATGGTCACGTGCATTGCGGTGGGGCTGCCCCTGCTGCTCATCTCGCTGGCCTTCGCGCAGGAGATCTCGA
TTGGTACACAGATAAGCTGTTTCTCTCCAAGTTCTTTCTCCTGGCGTCAGGCTGCCTTTGTGGATTCATATTGCTGGGCGGCTGTTCAG
CAGAAGAACTCACTGCAGAGCGAGTCTGGAAACCTCCCACTGTGGCTGCATAAGTTTTTCCCCTACATCCTGCTGCTCTTTGCGATCCT
CCTGTACCTGCCCCCGCTGTTCTGGCGTTTCGCAGCTGCTCCTCATATTTGCTCAGACTTGAAGTTTATCATGGAAGAACTTGACAAAG
TTTACAACCGTGCAATTAAGGCTGCAAAGAGTGCGCGTGACCTTGACATGAGAGATGGAGCCTGCTCAGTTCCAGGTGTTACCGAGAAC
TTAGGGCAAAGTTTGTGGGAGGTATCTGAAAGCCACTTCAAGTACCCAATTGTGGAGCAGTACTTGAAGACAAAGAAAAATTCTAATAA
TTTAATCATCAAGTACATTAGCTGCCGCCTGCTGACACTCATCATTATACTGTTAGCGTGTATCTACCTGGGCTATTACTTCAGCCTCT
                                  Panx1 siRNA 70
CCTCACTCTCAGACGAGTTTGTGTGCAGCATCAAATCAGGGATCCTGAGAAACGACAGCACCGTGCCCGATCAGTTTCAGTGCAAACTC
ATTGCCGTGGGCATCTTCCAGTTGCTCAGTGTCATTAACCTTGTGGTTTATGTCCTGCTGGCTCCCGTGGTTGTCTACACGCTGTTTGT
                                                                        Panx1 siRNA 7
TCCATTCCGACAGAAGACAGATGTTCTCAAAGTGTACGAAATCCTCCCCACTTTTGATGTTCTGCATTTCAAATCTGAAGGGTACAACG
ATTTGAGCCTCTACAATCTCTTCTTGGAGGAAAATATAAGTGAGGTCAAGTCATACAAGTGTCTTAAGGTACTGGAGAATATTAAGAGC
AGTGGTCAGGGGATCGACCCAATGCTACTCCTGACAAACCTTGGCATGATCAAGATGGATGTTGTTGATGGCAAAACTCCCATGTCTGC
AGAGATGAGAGAGGAGCAGGGGAACCAGACGGCAGAGCTCCAAGGTATGAACATAGACAGTGAAACTAAAGCAAATAATGGAGAGAAGA
                                  Panx1 siRNA 72
ATGCCCGACAGAGACTTCTGGATTCTTCTTGCTGA
```

B

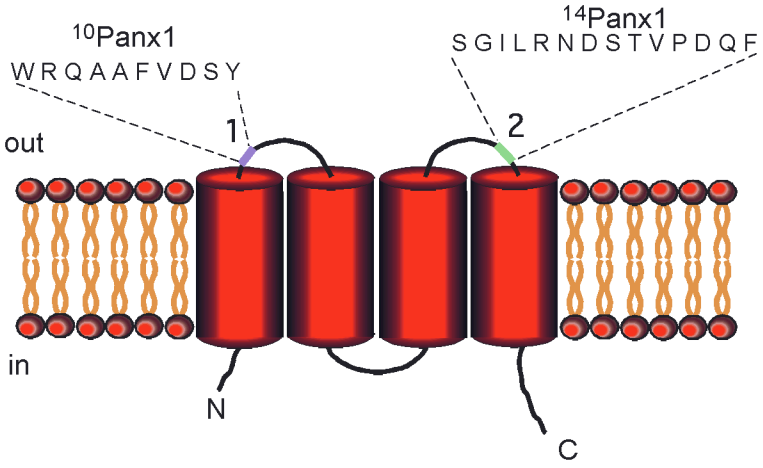

C

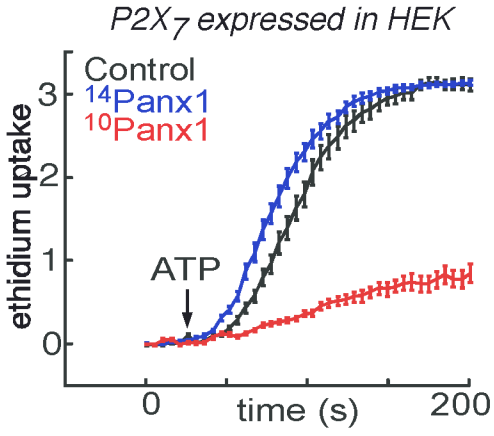

Supplementary Fig. 2